Histol Histopathol (2022) 37: 597-607

http://www.hh.um.es

Histology and Histopathology
From Cell Biology to Tissue Engineering

ORIGINAL ARTICLE **Open Access**

Fibroblast activation protein-alpha knockdown suppresses prostate cancer cell invasion and proliferation

Jiali An[1], Dingkun Hou[1], Lei Wang[1], Lili Wang[1], Yuanyuan Yang[1] and Haitao Wang[2]

[1]Tianjin Institute of Urology and [2]Department of Oncology, The Second Hospital of Tianjin Medical University, Tianjin, PR China

Summary. Background. Prostate cancer is one of the most common malignant tumors of the male genitourinary system. Fibroblast activation protein alpha (FAP-α) overexpression has been shown to occur in a wide range of tumors. However, the specific mechanism of FAP-α in the development of prostate cancer has not been reported.

Methods. In this study, real-time quantitative PCR (qRT-PCR) was used to detect the relative expression of FAP-α mRNA in prostate cancer cell lines (PC-3, LNCaP, and DU145) and human normal prostate epithelial cell line RWPE-1. Small interfering RNA (siRNA) targeting FAP-α and vectors expressing exogenous FAP-α were transfected to prostate cancer cells (LNCaP and DU145) to investigate the function of FAP-α. BALB/c nude mice were injected with DU145 cells which were transfected with NC-siRNA, FAP-α-siRNA-1, or FAP-α-siRNA-2.

Results. Compared to adjacent normal tissues, FAP-α protein and mRNA levels in prostate cancer tissues increased significantly ($P<0.05$). Compared to patients with high FAP-α mRNA levels, patients with low FAP-α mRNA levels had a significantly higher survival rate ($\chi^2=5.050$, log-rank $P=0.025$). Overexpression of FAP-α in LNCaP cells markedly inhibited cell apoptosis, and promoted cell invasion and proliferation. In contrast, knockdown of FAP-α expression in DU145 cells can significantly reduce invasion, proliferation, and promote apoptosis in prostate cancer. Immunofluorescence assay further indicated that down-regulation of FAP-α could suppress the nuclear translocation of β-catenin. An in vivo study found that compared with the NC-siRNA group, the tumor weight and tumor volume in the FAP-α-siRNA-1 and FAP-α-siRNA-2 groups were significantly decreased.

Conclusions. In conclusion, down-regulation of FAP-α can inhibit the invasion and proliferation of prostate cancer. Our study provides a theoretical basis for the targeted treatment of prostate cancer.

Key words: Prostate cancer, Fibroblast activation protein-alpha, Small interfering RNA, Invasion, Proliferation

Introduction

Prostate cancer is one of the most common primary malignant tumors among middle-aged and elderly people (Li et al., 2020a,b). The incidence of prostate cancer ranks second among all-male malignant tumors in the world, and the mortality rate ranks fifth (Bray et al., 2018). In recent years, with the aging of the Chinese population, the incidence of prostate cancer has been increasing year by year, and it has become the fifth most common malignant tumor in the male population (Ye and Zhu 2019). Endocrine therapy is currently the main treatment method for prostate cancer (Wang et al., 2009; Chandrasekar et al., 2015). Almost all patients are androgen-dependent in the early stage of the disease. The treatment remission rate of androgen deprivation therapy exceeds 80% (Wang et al., 2009). However, after a median survival period of 14 months, most patients develop castration-resistant prostate cancer, which becomes difficult to control and easy to metastasize (Chandrasekar et al., 2015). This is the main cause of death from advanced prostate cancer. Therefore, exploring the underlying molecular pathogenesis will help to guide the clinical treatment of prostate cancer.

Fibroblast activation protein alpha (FAP-α) is a type of serine protease, and it is also a regulator of mitosis necessary for cell proliferation (Shi et al., 2020). FAP-α plays a very important role in tumor disease progression,

Corresponding Author: Haitao Wang, Ph.D., Department of Oncology, The Second Hospital of Tianjin Medical University, 23 Pingjiang Road, Hexi District, Tianjin 300211, PR China. e-mail: wang_doc@21cn.com

DOI: 10.14670/HH-18-430

Abbreviations. CCK-8, cell counting kit-8; FAP-α, fibroblast activation protein-alpha; qRT-PCR, Real-time quantitative PCR; siRNA, small interfering RNA

cell infiltration, and metastasis (Teichgräber et al., 2015; Wu et al., 2020). Studies have found that FAP-α can be specifically expressed in tumor-associated fibroblasts and it can accelerate the growth and infiltration of tumor cells based on the protease hydrolysis reaction (Teichgräber et al., 2015; Shi et al., 2020; Wu et al., 2020). In addition, FAP-α can also accelerate the formation of new blood vessels and endothelial cells in tumor tissues and the metastasis of tumor cells (Martin-Padura et al., 2012). Besides, several studies have pointed out that the inhibition of FAP-α was an effective method for anticancer treatment (Teng et al., 2020; Yan et al., 2020). It is worth noting that a recent study described the up-regulation of FAP protein in castration-resistant prostate cancer (Kesch et al., 2021). The study also pointed out that increased FAP tissue expression supports the use of FAP inhibitor (FAPI)-molecular theranostics in castration-resistant prostate cancer (Kesch et al., 2021). Studies have shown that prostate cancer cells had high proliferative activity both in vitro and in vivo (Carpenter et al., 2020; Wang et al., 2020). This study intends to analyze the expression level of FAP-α in prostate cancer tissue samples. Furthermore, small interfering RNA (siRNA) and plasmid vectors were used to investigate the effect of FAP-α on invasion and proliferation in prostate cancer cells and tumor xenografts.

Materials and methods

Reagents and instruments

Human prostate cancer cell lines DU145 (NCBI_Iran Cat# C428, RRID: CVCL_0105), PC-3 (CLS Cat# 300312/p1699_PC-3, RRID: CVCL_0035), LNCaP (CLS Cat# 300265/p761_LNCaP, RRID: CVCL_0395) and human normal prostate epithelial cell line RWPE-1 (ATCC Cat# CRL-11609, RRID: CVCL_3791) were purchased from the Cell Bank of Tongji Medical College of Huazhong University of Science and Technology, China. RPMI1640 medium and 10% fetal bovine serum were purchased from Gibco, USA. The siRNA targeting FAP-α and the negative control (NC-siRNA) sequence were purchased from Invitrogen, USA. TRIZOL reagent and Lipofectamine 2000 were purchased from Shanghai Jingkang Biological Engineering Co., Ltd, China. Primer sequences were purchased from Wuhan Tianyi Huiyuan Biotechnology Co., Ltd, China.

Collection of prostate cancer tissue

The trial was conducted in accordance with the Declaration of Helsinki (2013). The study was approved by the Ethics Committee of The Second Hospital of Tianjin Medical University, Tianjin, China (NO.: LX201607-3), and informed consent was taken from all the patients. A total of 68 prostate cancer patients admitted to The Second Hospital of Tianjin Medical University from July 2016 to September 2018 were collected. All patients underwent surgery. Sixty-eight confirmed prostate cancer tissues and corresponding adjacent normal tissues were collected and stored in liquid nitrogen.

Postoperative follow-up of prostate cancer patients

According to the operation time, prostate cancer patients were followed up for 24 months, and the number of deaths and the corresponding death time during the follow-up period were counted.

Cell culture

DU145, PC-3, LNCaP, and RWPE-1 cell lines were cultured in RPMI1640 medium. 10% fetal bovine serum was added to the medium and cultured in a 37°C saturated humidity incubator containing 5% CO_2.

Cell transfection

DU145 and LNCaP cells were seeded into a 24-well plate at 1×10^5 cells per well. Lipofectamine 2000 was used to transfect FAP-α-siRNA and NC-siRNA into DU145 cells, and transfect pcDNA-FAP-α plasmid and NC plasmid into LNCaP cells (Blersch et al., 2020; Li et al., 2020a,b). After 24h of transfection, the collected cells were used for subsequent experiments.

Western blotting

Each protein sample (50 μg) was separated by 10% polyacrylamide gel electrophoresis and electrophoresed onto a polyvinylidene fluoride membrane. Next, the membrane was incubated with anti-FAP-α (MBL International Cat# LS-A8025, RRID: AB_843099), anti-N-cadherin (G.R. Phillips, Mount Sinai School of Medicine; New York; USA Cat# N-cadherin, RRID: AB_2314843), anti-E-cadherin (Thermo Fisher Scientific Cat# 51-3249-82, RRID: AB_1210532), anti-β-catenin (Cell Signaling Technology Cat# 8480, RRID: AB_11127855), anti-Vimentin (EnCor Biotechnology Cat# RPCA-Vim, RRID: AB_2572398), anti-Snail (LifeSpan Cat# LS-C97986-100, RRID: AB_10559089), anti-Bax (GenWay Biotech Inc. Cat# 18-661-15197-0.1 mg, RRID: AB_516294), anti-ki-67 (EnCor Biotechnology Cat# RPCA-Ki67, RRID: AB_2637050), and anti-glyceraldehyde-3-phosphate dehydrogenase (GAPDH, MBL International Cat# JM-3777-100, RRID:AB_843142) antibodies overnight. Finally, the secondary antibody was incubated for 2 hours, and the gray band of the protein band was detected by chemiluminescence.

Quantitative real-time PCR (qRT-PCR)

Total RNAs from tissue homogenates (100 mg) and cell lines were extracted using the TRIZOL method and

were reverse-transcribed into cDNA. QRT-PCR was performed in 20 μL system, including 2X Mix SYBR green I (10 μL), upstream and downstream primers (0.5 μL each), cDNA (2 μL), and sterile water (7 μL). The $2^{-\Delta\Delta Ct}$ method was used to calculate the relative expression of the target gene. The primer against FAP-α was 5'-AATGTGGCATAGCAGTGGCT-3' (forward) and 5'-TGTTGGGAGGCCCATGAATC-3' (reverse). The primer against GAPDH was 5'-AACTTTGGCA TTGTGGAAGG-3' (forward) and 5'-GGATGCAGG GATGATGTTCT-3' (reverse).

Transwell assay

2×10^5 cells in serum-free medium were seeded into the Matrigel-coated Transwell upper chamber. RPMI-1640 containing 10% fetal bovine serum was added to the lower chamber. After 24 hours, the membrane containing the invading cells was gently removed and mounted on a glass slide, the glass slide was fixed with 4% formaldehyde for 20 min and stained with 0.1% crystal violet. The cells were photographed at 200X magnification with an inverted optical microscope, and the number of cells in 10 fields was randomly counted.

Cell counting kit-8 (CCK-8) assay

In each group, 5×10^3 cells were seeded in 96-well plates, and 10 uL of CCK-8 solution was added to each well at different time points (0 h, 24 h, 48 h, and 72 h) and cultured for 2h. An enzyme-linked immunosorbent assay was used to determine the optical density (A) at a wavelength of 570 nm. All experiments were repeated three times.

Clone formation experiment

Transfected cells were plated in 96-well plates. After the cells adhered, the transfected cells were cultured for 48 h. After washing gently with phosphate-buffered saline (PBS) twice, it was fixed with 4% paraformaldehyde for 10 min, and stained with Giemsa stain for 15 min.

Immunohistochemistry

Tissue paraffin sections were fixed in an oven at 60°C for 2 h. To avoid nonspecific links, the incisions were rinsed with TBS before adding the primary antibody. After the calf serum was blocked for 30 min, rabbit anti-human FAP-α (1: 2000) was added. The secondary antibody was incubated at 37°C for 30 min, rinsed with PBS. Two independent pathologists, who were not given the clinical information, evaluated the immunoreaction, specifying the percentage of positive colored cancer cells. Differences were resolved with consensus. FAP-α positive prostate cancer cells were defined as brown membranous and cytoplasmic staining. Positively stained cells were counted in five randomly selected fields at magnification of×400. In addition, we separately detected the immunohistochemical level of FAP-α protein in stromal cells and epithelial cells. Proportion, intensity, and combined score were evaluated. The frequency of positive cells was defined as follow: 0, less than 5%; 1, 5% to 25%; 2, 26% to 50%; 3, 51% to 75%; and 4, greater than 75%. The intensity was scored as follows: 0, negative; 1, weak; 2, moderate; and 3, strong. An overall score of 0 to 12 (product of proportion and intensity) was calculated for each specimen (Striefler et al., 2021). In this study, we defined a score of ≤7 as low expression, and a score greater than 7 as high expression.

Flow cytometry for apoptosis and mitochondrial membrane potential

Cultured cells were digested with trypsin. After being mixed with 5 uL of Annexin V-FITC fluorescent dye, they were incubated for 15 min at room temperature. Then, 5 μL of Propidium Iodide (PI) fluorescent dye was added, and the apoptosis of each group was observed at 488 nm.

Analysis of mitochondrial membrane potential was performed using a JC-1 staining kit (Thermo Fisher Scientific, USA). Cultured cells were incubated with staining buffer at 5 μM concentration at 37°C for 30 min. Then, stained cells were analyzed using a flow cytometer.

Immunofluorescence analysis

Five groups of transfected cells were seeded in eight-well chamber slides and cultured overnight. After washing with 1×PBS medium, cells were fixed with pre-cooled methanol for 15 min at -20°C. Then the cells were blocked in 5% donkey serum for 45 min at room temperature. After incubation with the primary antibody in 1×PBS at 4°C overnight, the cells were washed with 1×PBS and incubated with a secondary antibody in 1×PBS for 45 min. Then cells were washed and stained with DAPI for 10 min and observed by a fluorescence microscope.

Tumor xenograft

Eighteen BALB/c nude mice (IMSR Cat# ORNL: BALB/c-PF, RRID: IMSR_ORNL: BALB/c-PF) of SPF grade were purchased from the Experimental Animal Center of Tianjin Medical University [SCXK (E) 2019-0134]. Experiments were performed under a project license (NO.: 20190408-3) granted by the Experimental Animal Center of Tianjin Medical University, in compliance with the Experimental Animal Center of Tianjin Medical University guidelines for the care and use of animals. Humane care was given during the experimental animal breeding and experimental procedures following the 3R principle of experimental animals. The three groups of cells treated with FAP-α-

siRNA-1, FAP-α-siRNA-2, and NC-siRNA were cultured for 24 h. 4×10^6 cells were subcutaneously inoculated into nude mice (6 nude mice were inoculated in each group). Tumor weight and tumor volume were measured with calipers after 4 weeks.

Statistical analysis

Statistical analysis was performed using SPSS 20.0 (SPSS, RRID: SCR_002865). The measurement data were expressed as mean ± standard deviation (SD). T-test was used for comparison between two groups. Correlation analysis was performed using the Pearson method. Survival curve analysis was performed using the Kaplan-Meier method. $P<0.05$ was considered statistically significant.

Results

Expression of FAP-α in prostate cancer tissues and its relationship with patients' clinical characteristics and prognosis

A total of 68 pairs of prostate cancer tissues and adjacent normal tissues were collected in the current study. Immunohistochemical staining results are shown in Fig. 1A. There was no statistically significant difference in the immunohistochemical level of FAP-α protein in stromal cells between cancer and adjacent normal tissues (P=0.419). Compared with adjacent normal tissues, FAP-α protein in prostate cancer tissues increased significantly (P<0.05). We divided patients into two groups (FAP-α immunohistochemical score ≤7

Table 1. Relationship between FAP-α immunohistochemical score and clinicopathological characteristics in prostate cancer tissue.

Groups	FAP-α immunohistochemical score ≤7 (n=43)	FAP-α immunohistochemical score >7 (n=25)	χ^2	P
Age			0.093	0.761
<60	24	13		
≥60	19	12		
Tumor size			10.463	0.001
≥1.5 cm	17	20		
<1.5 cm	26	5		
Differentiation status			0.325	0.569
Well	21	14		
Moderate-poor	22	11		
Invasion depth			11.944	0.001
T1-T2	29	6		
T3-T4	14	19		

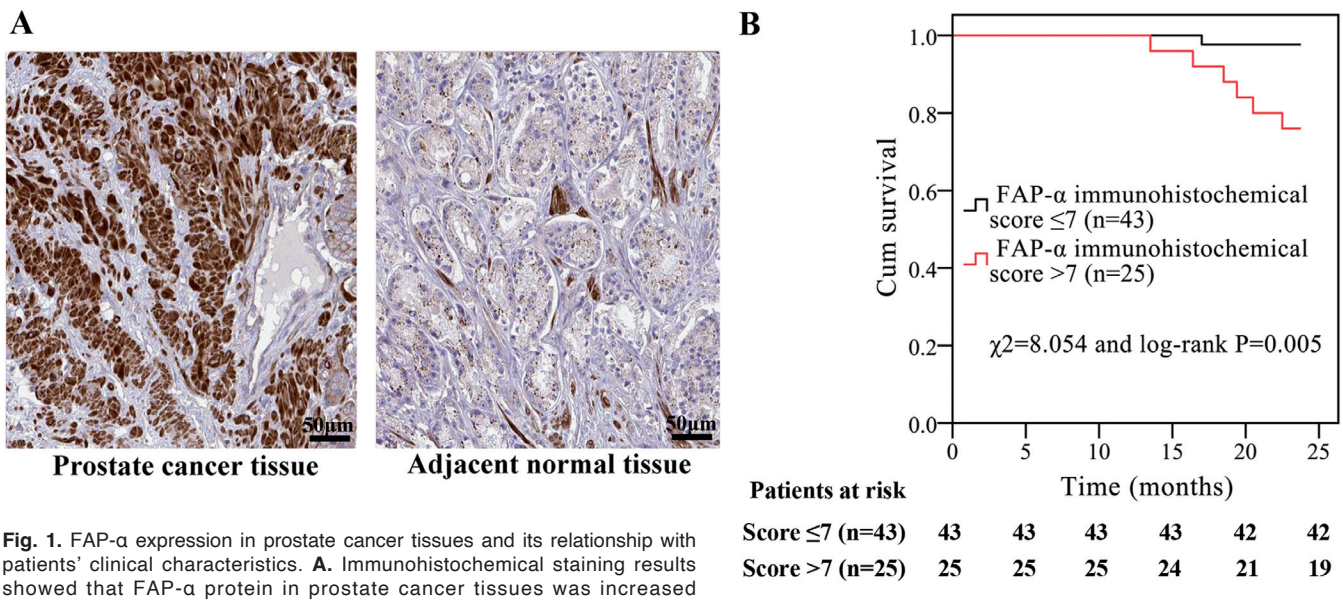

Fig. 1. FAP-α expression in prostate cancer tissues and its relationship with patients' clinical characteristics. **A.** Immunohistochemical staining results showed that FAP-α protein in prostate cancer tissues was increased significantly compared to the adjacent normal tissues. **B.** Compared to patients with high FAP-α immunohistochemical score, patients with low FAP-α immunohistochemical score had a significantly higher two-year survival rate (χ2=8.054 and log-rank P=0.005). Scale bars: 50 μm.

and FAP-α immunohistochemical score >7) according to the FAP-α immunohistochemical score in prostate cancer tissue. Compared to the patients with a high FAP-α immunohistochemical score, patients with low FAP-α immunohistochemical score had a significantly higher two-year survival rate (χ^2=8.054 and log-rank P=0.005, Fig. 1B). FAP-α immunohistochemical score in prostate cancer tissue was positively correlated with tumor size and invasion depth (P<0.05, Table 1). Cox analysis showed that the FAP-α immunohistochemical score, tumor size, and invasion depth were all risk factors for postoperative death in prostate cancer patients (P<0.05, Table 2).

Expression of FAP-α in prostate cancer cell lines and the verification of FAP-α gene silencing and overexpressing

As shown in Fig. 2A, the mRNA levels of FAP-α were significantly increased in LNCaP, DU145, and PC-3 cell lines compared to those in the RWPE-1 cell line (P<0.05). Further, we verified the transfection efficiency of pcDNA-FAP-α (in LNCaP cell line) and FAP-α-siRNA (in DU145 cell line). Compared with the NC-pcDNA group, the protein level of FAP-α in the pcDNA-FAP-α-1 group was significantly increased (P<0.05, Fig. 2B). Compared with the NC-siRNA group, the protein levels of FAP-α in the FAP-α-siRNA-1 and FAP-α-

Table 2. Cox proportional regression model analysis of risk factors for death in prostate cancer patients.

	β	SE	Wald χ^2	P	HR	95%CI
Age	0.099	0.067	2.156	0.147	1.109	0.964~1.293
Tumor size	**0.181**	**0.064**	**7.737**	**0.006**	**1.184**	**1.061~1.364**
Differentiation status	0.023	0.086	0.059	0.829	1.020	0.876~1.243
Invasion depth	**0.369**	**0.029**	**18.409**	**<0.001**	**1.495**	**1.247~1.773**
FAP-α immunohistochemical score	**0.195**	**0.097**	**8.352**	**0.006**	**1.153**	**1.057~1.316**

β, regression coefficients; CI, confidence interval; HR, hazard ratio; SE, standard error. Bold characters indicate significant differences.

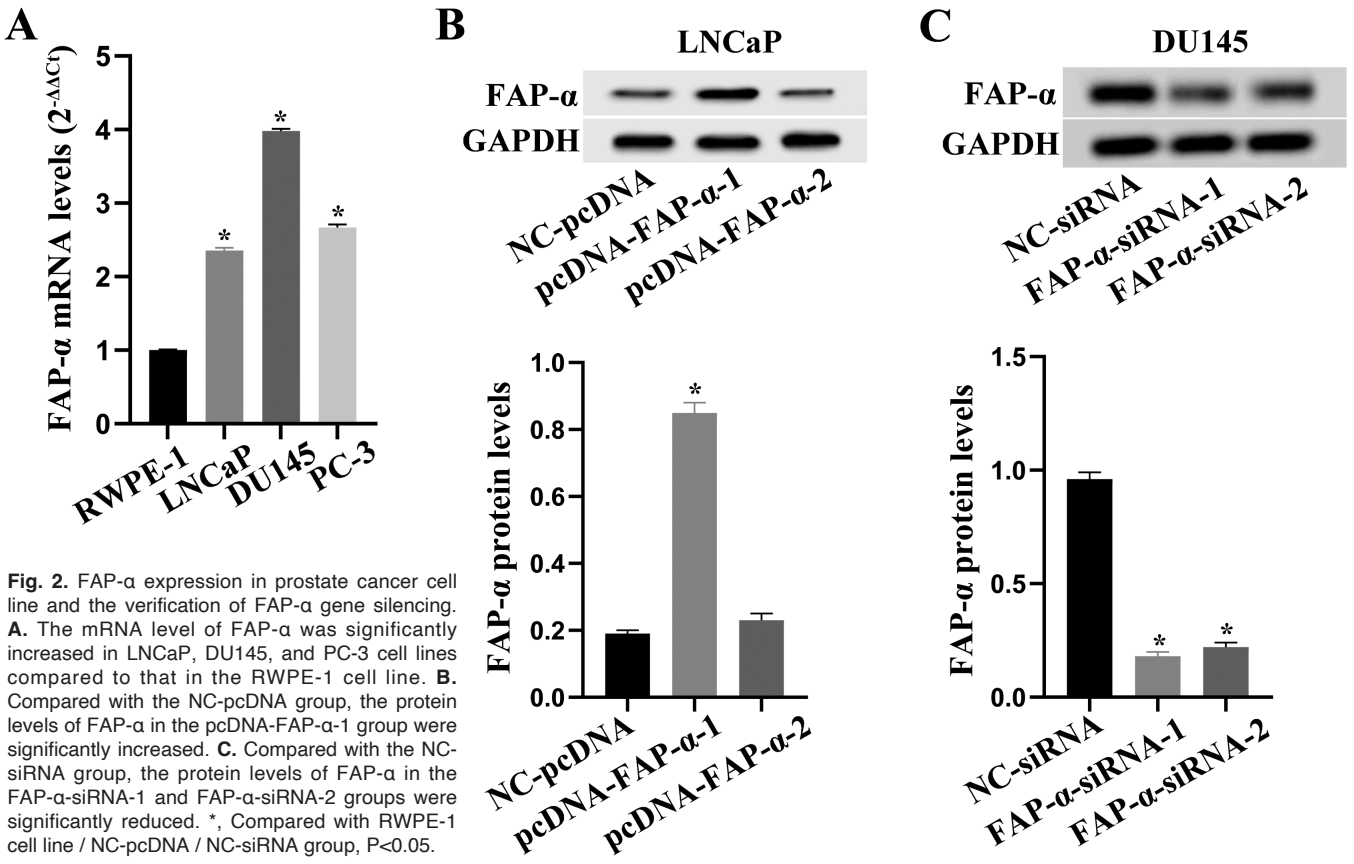

Fig. 2. FAP-α expression in prostate cancer cell line and the verification of FAP-α gene silencing. **A.** The mRNA level of FAP-α was significantly increased in LNCaP, DU145, and PC-3 cell lines compared to that in the RWPE-1 cell line. **B.** Compared with the NC-pcDNA group, the protein levels of FAP-α in the pcDNA-FAP-α-1 group were significantly increased. **C.** Compared with the NC-siRNA group, the protein levels of FAP-α in the FAP-α-siRNA-1 and FAP-α-siRNA-2 groups were significantly reduced. *, Compared with RWPE-1 cell line / NC-pcDNA / NC-siRNA group, P<0.05.

siRNA-2 groups were significantly reduced (P<0.05, Fig. 2C). Therefore, pcDNA-FAP-α-1, FAP-α-siRNA-1, and FAP-α-siRNA-2 were selected for subsequent experiments.

FAP-α promotes the invasion and proliferation and inhibits apoptosis of prostate cancer cells

Results showed that the invasion and proliferation levels were increased, and the apoptosis level was decreased in LNCaP cells treated with pcDNA-FAP-α (Fig. 3A-C). Moreover, overexpression of FAP-α promoted the epithelial-mesenchymal transition (EMT) of LNCaP by inhibiting E-cadherin expression and increasing Vimentin, β-catenin, N-cadherin, and Snail expressions (Fig. 3D). Previous studies found that FAP-α was able to promote β-catenin nuclear translocation (Ren et al., 2016). Therefore, we detected the nucleic location of β-catenin after the transfection of the FAP-α inhibitor by immunofluorescence assay. We found that pcDNA-FAP-α was able to promote the nuclear translocation of β-catenin (P<0.05, Fig. 3E).

Silencing FAP-α inhibits DU145 cell invasion and EMT

Since FAP-α mRNA expressed most highly in the DU145 cell line, DU145 was selected for subsequent transfection experiments. Results from the transwell assay suggested that transfection with FAP-α-siRNA-1 or FAP-α-siRNA-2 significantly suppressed the invasion of DU145 cells compared with the NC-siRNA group (P<0.05, Fig. 4A). Next, we detected N-cadherin, E-cadherin, β-catenin, Vimentin, and Snail expressions by western blot assay. Our results suggested that the E-cadherin expression was significantly increased after transfection with FAP-α-siRNA-1 and FAP-α-siRNA-2, while the N-cadherin, β-catenin, Vimentin, and Snail expressions were significantly decreased (P<0.05, Fig. 4B). Moreover, we found that FAP-α-siRNA-1 and FAP-α-siRNA-2 was able to suppress the nuclear translocation of β-catenin (P<0.05, Fig. 4C). Together, these findings implied that FAP-α might promote DU145 cell invasion.

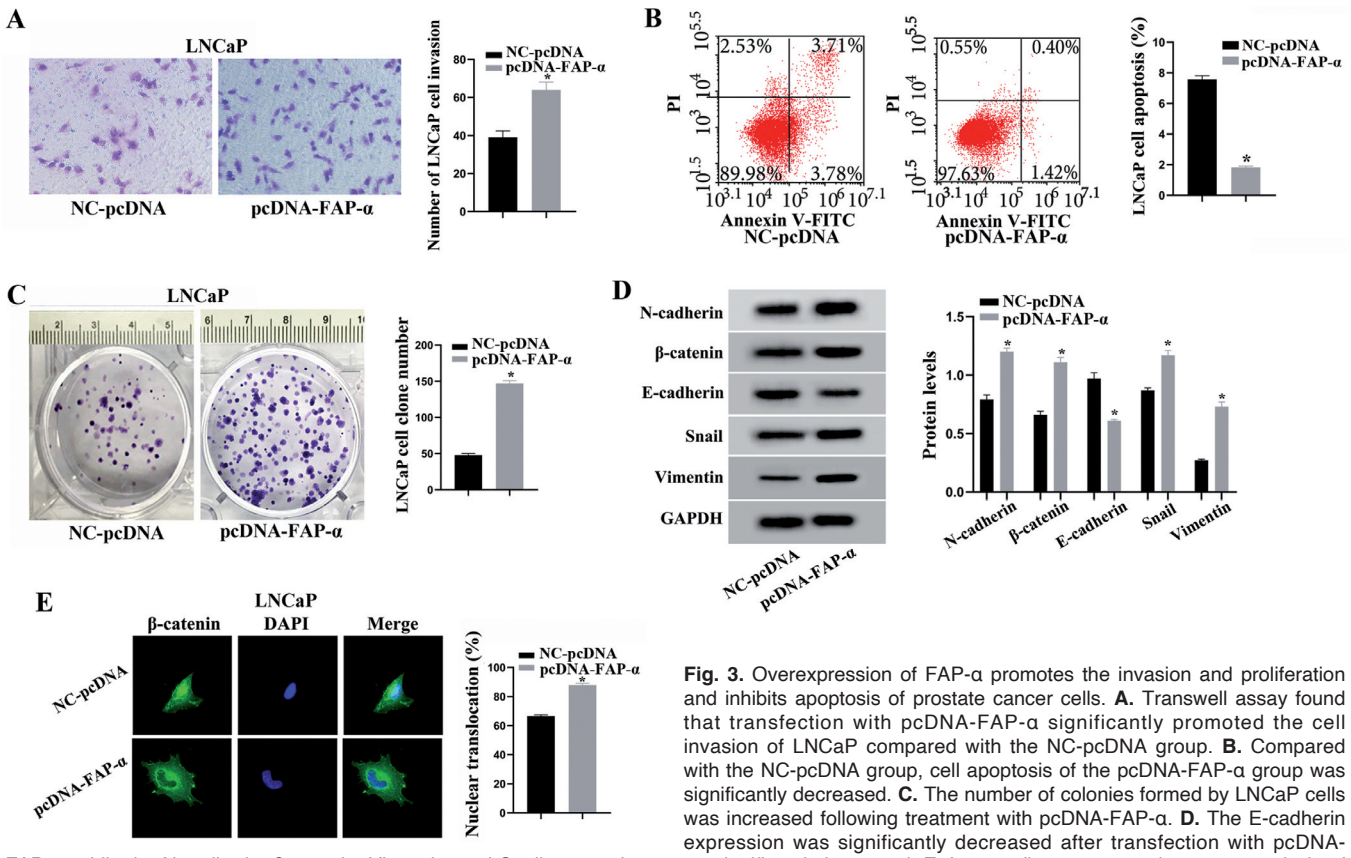

Fig. 3. Overexpression of FAP-α promotes the invasion and proliferation and inhibits apoptosis of prostate cancer cells. **A.** Transwell assay found that transfection with pcDNA-FAP-α significantly promoted the cell invasion of LNCaP compared with the NC-pcDNA group. **B.** Compared with the NC-pcDNA group, cell apoptosis of the pcDNA-FAP-α group was significantly decreased. **C.** The number of colonies formed by LNCaP cells was increased following treatment with pcDNA-FAP-α. **D.** The E-cadherin expression was significantly decreased after transfection with pcDNA-FAP-α, while the N-cadherin, β-catenin, Vimentin, and Snail expressions were significantly increased. **E.** Immunofluorescence microscopy analysis of β-catenin nuclear translocation in LNCaP cells following transfection with pcDNA-FAP-α and NC-pcDNA. *, Compared with the NC-pcDNA group, P<0.05. A, x 400.

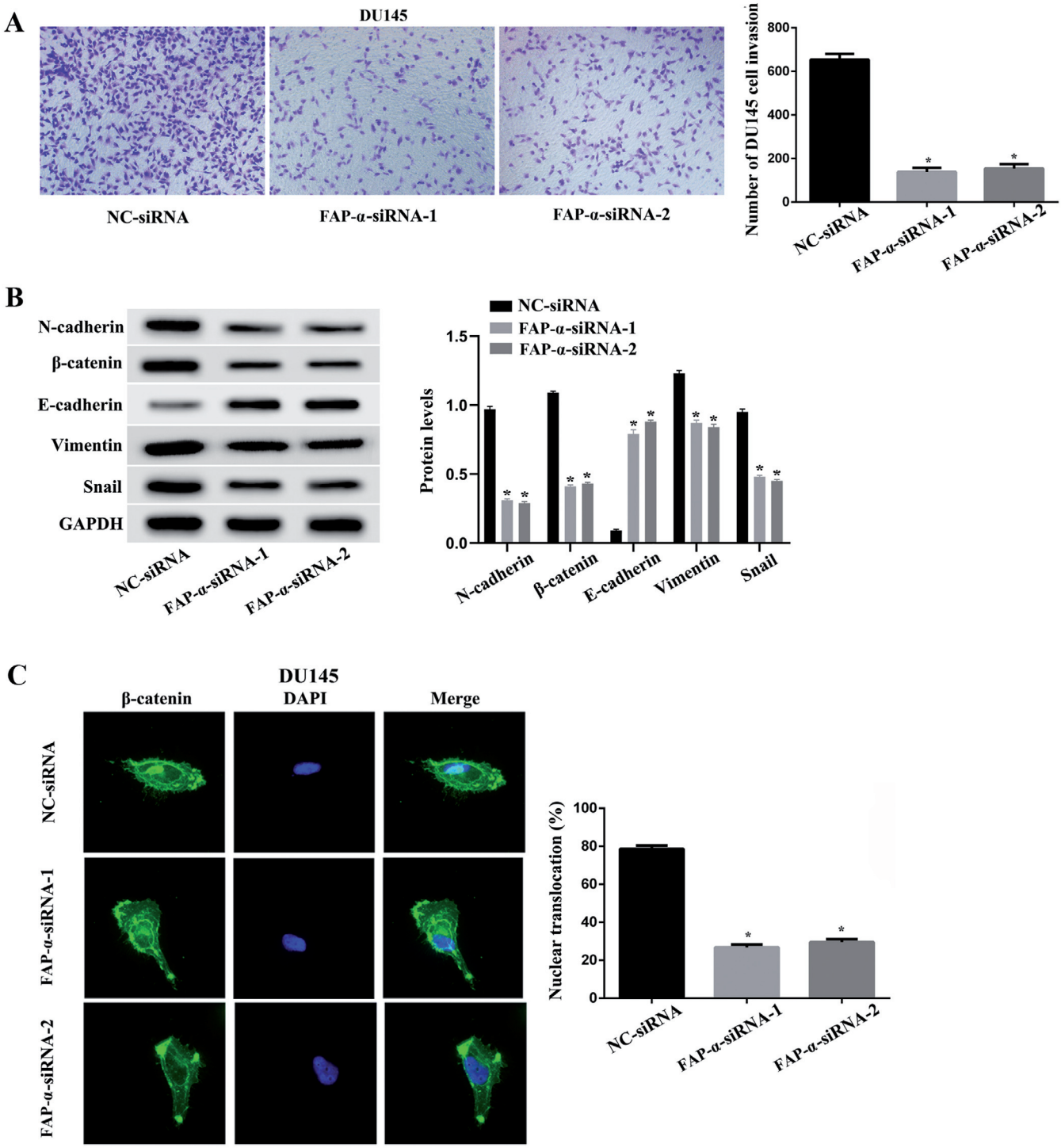

Fig. 4. Silencing FAP-α inhibits DU145 cell invasion. **A.** Transwell assay found that transfection with FAP-α-siRNA-1 or FAP-α-siRNA-2 significantly suppressed the cell invasion of DU145 compared with the NC-siRNA group. **B.** E-cadherin expression was significantly increased after transfection with FAP-α-siRNA-1 and FAP-α-siRNA-2, while N-cadherin, β-catenin, Vimentin, and Snail expressions were significantly decreased. **C.** Immunofluorescence microscopy analysis of β-catenin nuclear translocation in DU145 cells following transfection with FAP-α inhibitor and NC-siRNA. *, Compared with the NC-siRNA group, P<0.05. A, x 200.

Silencing FAP-α inhibits DU145 cell proliferation

The capacity for cell apoptosis was determined using the flow cytometry assay. The effect of FAP-α on apoptosis of DU145 cells is shown in Fig. 5A. Compared with the NC-siRNA group, cell apoptosis in the FAP-α-siRNA-1 and FAP-α-siRNA-2 groups were significantly increased ($P<0.05$). To investigate the functional roles of FAP-α in DU145 cell proliferation, clone formation experiments, CCK-8, and western blot assays were performed. We found that the number of colonies formed by DU145 cells was reduced following the treatment of FAP-α-siRNA-1 or FAP-α-siRNA-2 ($P<0.05$, Fig. 5B). CCK-8 results are shown in Fig. 5C. At 0h, there was no significant difference in the proliferation capacity of DU145 cells among the NC-siRNA, FAP-α-siRNA-1, and FAP-α-siRNA-2 groups ($P>0.05$). However, at 24h, 48h, and 72h, compared with the NC-siRNA group, the cell proliferation ability in FAP-α-siRNA-1 and FAP-α-siRNA-2 groups were significantly reduced ($P<0.05$).

The result of the western blot showed that inhibiting FAP-α expression suppressed ki-67 expression and promoted Bax expression in DU145 cells ($P<0.05$, Fig. 6A). As shown in Fig. 6B, the inhibition of FAP-α increased the proportion of green staining. Our data showed that FAP-α-siRNA inhibited the mitochondrial transmembrane potential ($\Delta\Psi m$), which in turn promoted apoptosis. Overall, these results indicated that the inhibition of FAP-α reduced proliferation and promoted apoptosis of DU145 cells.

Silencing FAP-α inhibits prostate cancer growth in vivo

To determine the role of FAP-α in prostate cancer progression in vivo, BALB/c nude mice were injected with DU145 cells which were transfected with NC-siRNA, FAP-α-siRNA-1, or FAP-α-siRNA-2. Compared with the NC-siRNA group, the tumor weight and tumor volume in the FAP-α-siRNA-1 and FAP-α-siRNA-2

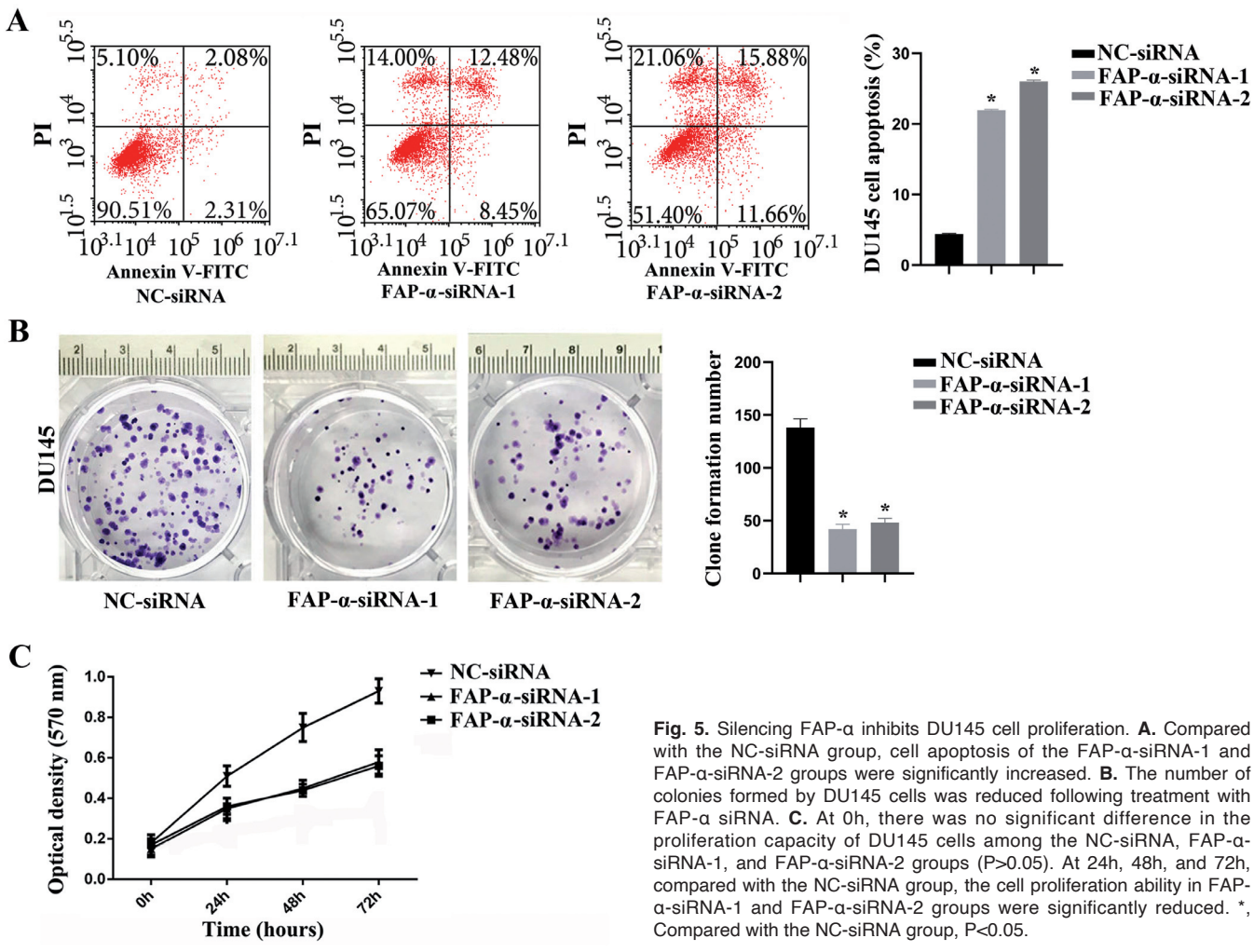

Fig. 5. Silencing FAP-α inhibits DU145 cell proliferation. **A.** Compared with the NC-siRNA group, cell apoptosis of the FAP-α-siRNA-1 and FAP-α-siRNA-2 groups were significantly increased. **B.** The number of colonies formed by DU145 cells was reduced following treatment with FAP-α siRNA. **C.** At 0h, there was no significant difference in the proliferation capacity of DU145 cells among the NC-siRNA, FAP-α-siRNA-1, and FAP-α-siRNA-2 groups ($P>0.05$). At 24h, 48h, and 72h, compared with the NC-siRNA group, the cell proliferation ability in FAP-α-siRNA-1 and FAP-α-siRNA-2 groups were significantly reduced. *, Compared with the NC-siRNA group, $P<0.05$.

groups were significantly decreased (P<0.05, Fig. 7A-C). Western blot assay has shown that the FAP-α protein levels in FAP-α-siRNA-1 and FAP-α-siRNA-2 groups were significantly decreased compared to those in the NC-siRNA group (P<0.05, Fig. 7D).

Discussion

FAP-α overexpression has been shown to occur in a wide range of tumors, prompting research and development of FAP-α inhibitors for cancer treatment (Teichgräber et al., 2015; Teng et al., 2020; Wu et al., 2020; Yan et al., 2020). Yang et al. (2018) pointed out that microRNA-204 was able to inhibit the malignant biological process of glioblastoma by inhibiting FAP-α expression. Their study also suggested that FAP-α could be inhibited by targeting microRNA-204 expression in patients with glioblastoma. In this study, we down-regulated the expression of FAP-α by transfecting FAP-α-siRNA into DU145 cells and observed its effect on the invasion and proliferation capacity of DU145 cells. Moreover, DU145 cells transfected with FAP-α-siRNA were inoculated into BALB/c nude mice to further observe the effect of FAP-α on the development of prostate cancer. Our results indicated that silencing FAP-α expression was able to significantly inhibit the invasion and proliferation of prostate cancer.

In this study, our results showed that the FAP-α protein levels were up-regulated in prostate cancer tissues compared with the adjacent normal tissues, and patients with low FAP-α levels had a significantly higher survival rate. Moreover, FAP-α mRNA levels were also up-regulated in prostate cancer cell lines compared with the RWPE-1 cell line. We found that the inhibition of FAP-α significantly promoted prostate cancer cell apoptosis and inhibited proliferation compared to cells transfected with NC-siRNA. In contrast, exogenous expression of FAP-α markedly inhibited the apoptosis but promoted the proliferation of prostate cancer cells. Our research results are consistent with previous research findings (Wu et al., 2020). Wu et al. (2020) found that the inhibition of FAP-α was able to alleviate fibroblast activation in pulmonary fibroblast cells. In this study, in order to clearly show the effect of FAP-α on the nuclear translocation of β-catenin, we performed a subcellular fraction analysis. Invasion is one process of metastasis (Williams et al., 2019). Here, our data indicated that decreased FAP-α levels significantly inhibited the invasive ability of DU145 cells compared with the NC-siRNA group. The EMT process has been

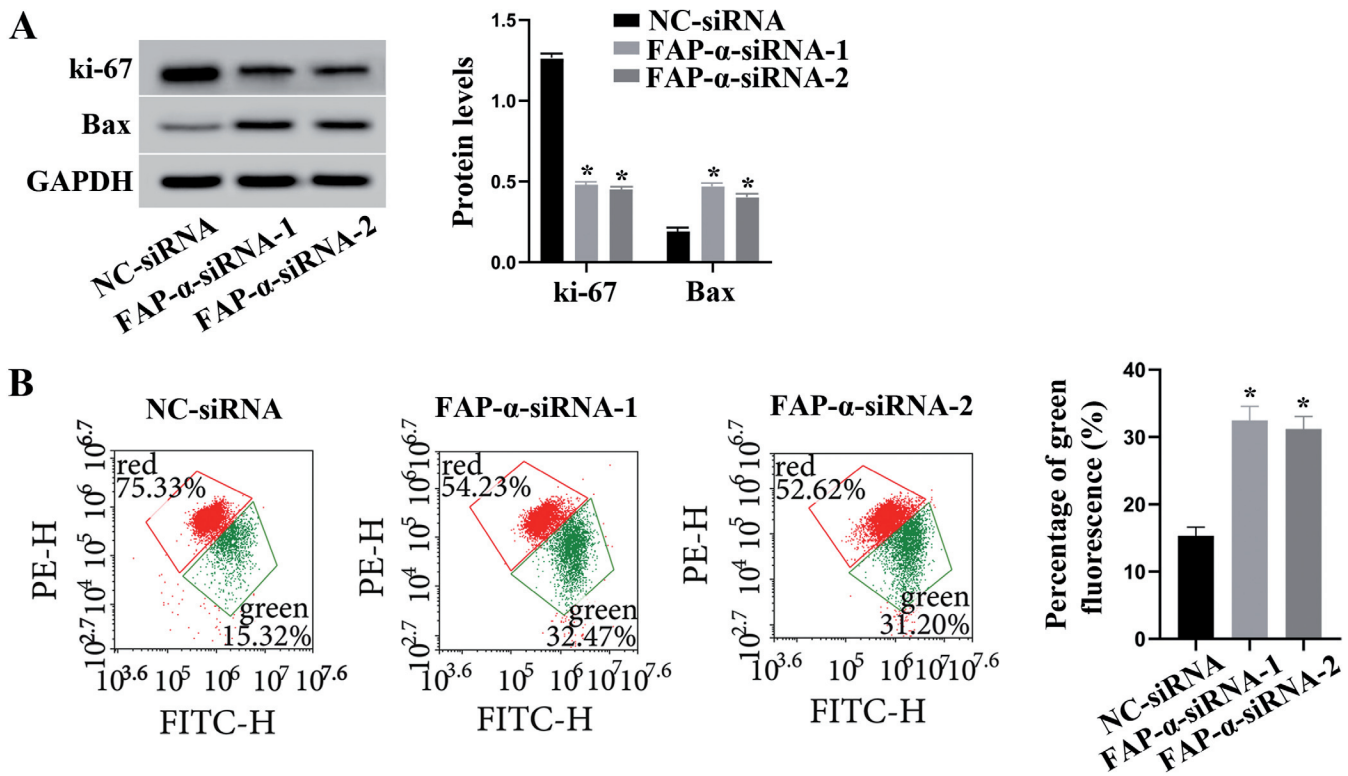

Fig. 6. FAP-α regulates mitochondrial membrane potential and related proteins. **A.** Inhibition of FAP-α expression in DU145 down-regulated ki-67 levels and up-regulated Bax expression. **B.** JC-1 staining was used to determine the mitochondrial transmembrane potential (ΔΨm). JC-1 is normally visualized as green when ΔΨm is reduced. *, Compared with the NC-siRNA group, P<0.05.

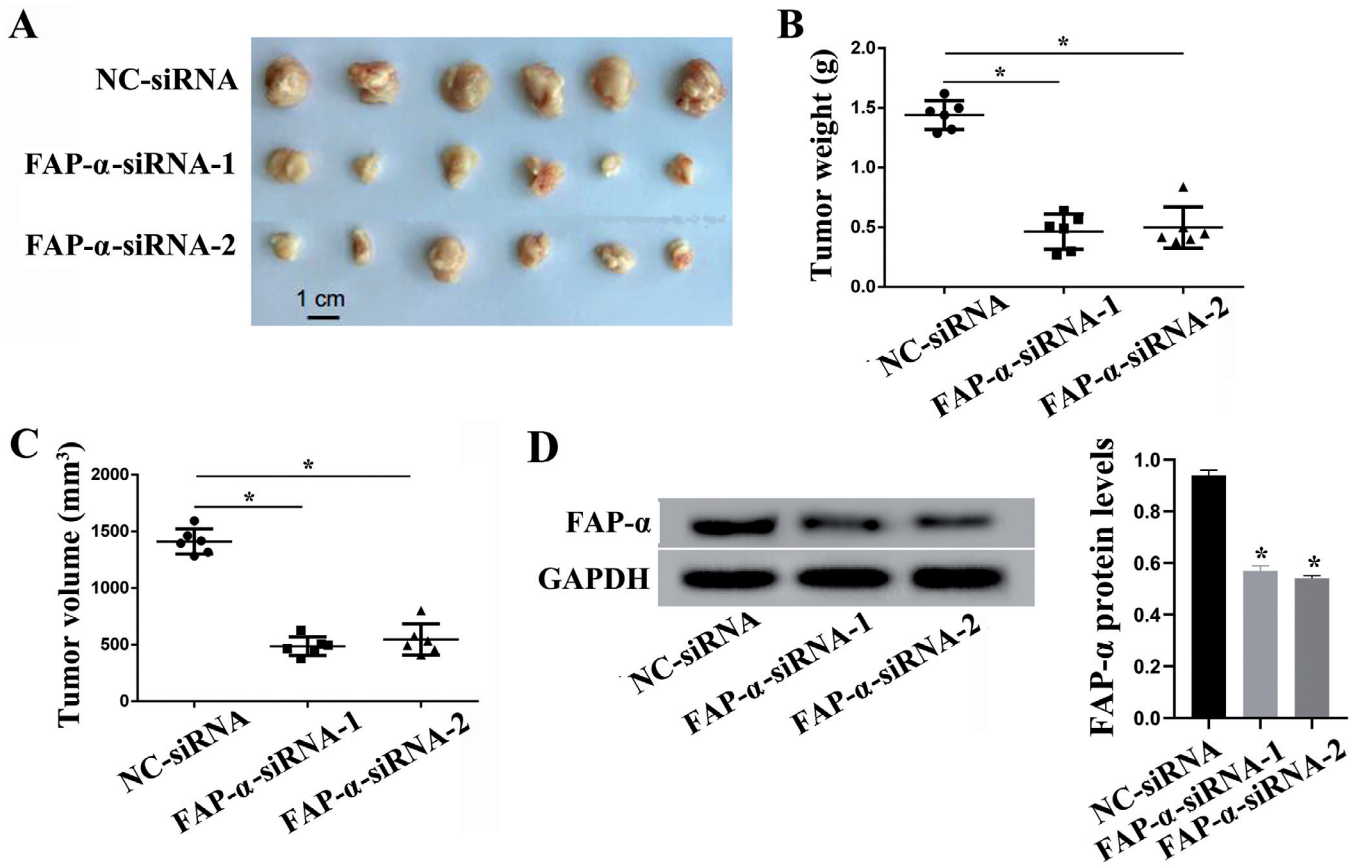

Fig. 7. Silencing FAP-α inhibits prostate cancer growth *in vivo*. **A-C.** Compared with the NC-siRNA group, the tumor weight and tumor volume in the FAP-α-siRNA-1 and FAP-α-siRNA-2 groups were significantly decreased. **D.** Compared with the NC-siRNA group, the protein levels of FAP-α in the FAP-α-siRNA-1 and FAP-α-siRNA-2 groups were significantly reduced. *, Compared with the NC-siRNA group, $P<0.05$.

confirmed to be critical in cell invasion in different types of cancer (Pastushenko and Blanpain, 2019). At the molecular level, EMT is characterized by down-regulation of epithelial marker E-cadherin, with up-regulation of mesenchymal markers like N-cadherin, β-catenin, Vimentin, and Snail (Radice, 2013; Ma et al., 2018). We found that inhibition of FAP-α suppressed the EMT of prostate cancer cells by increasing E-cadherin and decreasing N-cadherin, β-catenin, Vimentin, and Snail expressions. All the above results indicated that the down-regulation of FAP-α restrained cell proliferation, invasion, and EMT of prostate cancer. In addition, we explored the association between FAP-α and prostate cancer using the data obtained from human research and in vivo studies. BALB/c nude mice inoculated subcutaneously with DU145 cells treated with FAP-α-siRNA had a significantly reduced tumor weight and tumor volume.

This study still has the following shortcomings: (1) In this study, we used the clinical data and the follow-up information from only 68 cases of prostate cancer patients, so our conclusions need to be verified by a larger sample size study. (2) The prostate cancer patients collected in this study are all from our hospital, which may easily affect the accuracy of the results due to sample selection bias. Therefore, more multi-center, large-sample studies are needed to verify our findings. In conclusion, our results suggest that the down-regulation of FAP-α can inhibit the invasion and proliferation of prostate cancer, which provides a theoretical basis for the targeted prevention and treatment of prostate cancer.

Acknowledgements. This study was funded by the Zhejiang Province Public Welfare Technology Application Research Project (LGF21H160028).

Conflict of interest statement. none declared.

References

Bray F., Ferlay J., Soerjomataram I., Siegel R.L., Torre L.A. and Jemal A. (2018). Global cancer statistics 2018: GLOBOCAN estimates of incidence and mortality worldwide for 36 cancers in 185 countries. CA. Cancer J. Clin. 68, 394-424.

Blersch, J., Francisco, V., Rebelo, C., Jiménez-Balsa, A., Antunes, H., Pinto, S., Simões, S., Rai, A. and Ferreira L. (2020). A light-

triggerable formulation to control the stability of pro-angiogenic transcription factor hypoxia inducible factor-1α (HIF-1α). Nanoscale 12, 9935-9942.

Carpenter V.J., Patel B.B., Autorino R., Smith S.C., Gewirtz D.A. and Saleh T. (2020). Senescence and castration resistance in prostate cancer: A review of experimental evidence and clinical implications. Biochim. Biophys. Acta Rev. Cancer 1874, 188424.

Chandrasekar T., Yang J.C., Gao A.C. and Evans C.P. (2015). Mechanisms of resistance in castration-resistant prostate cancer (CRPC). Transl. Androl. Urol. 4, 365-380.

Kesch, C., Yirga, L., Dendl, K., Handke, A., Darr, C., Krafft, U., Radtke, J. P., Tschirdewahn, S., Szarvas, T., Fazli, L., Gleave, M., Giesel, F. L., Haberkorn, U. and Hadaschik, B. (2021). High fibroblast-activation-protein expression in castration-resistant prostate cancer supports the use of FAPI-molecular theranostics. Eur. J. Nucl. Med. Mol. Imaging 49, 385-389.

Li W., Dong Y., Wang K.J., Deng Z., Zhang W. and Shen H.F. (2020a). Plasma exosomal miR-125a-5p and miR-141-5p as non-invasive biomarkers for prostate cancer. Neoplasma 67, 1314-1318.

Li J., Song Y., Yu B. and Yu Y. (2020b). TNFAIP2 Promotes Non-Small Cell Lung Cancer Cells and Targeted by miR-145-5p. DNA Cell Biol. 39, 1256-1263.

Martin-Padura I., Gregato G., Marighetti P., Mancuso P., Calleri A., Corsini C., Pruneri G., Manzotti M., Lohsiriwat V., Rietjens M., Petit J. Y. and Bertolini F. (2012). The white adipose tissue used in lipotransfer procedures is a rich reservoir of CD34+ progenitors able to promote cancer progression. Cancer Res. 72, 325-334.

Ma J. Zhang J., Weng Y.C. and Wang J.C. (2018). EZH2-mediated microRNA-139-5p regulates epithelial-mesenchymal transition and lymph node metastasis of pancreatic cancer. Mol. Cells 41, 868-880.

Pastushenko I. and Blanpain C. (2019). EMT transition states during tumor progression and metastasis. Trends. Cell Biol. 29, 212-226.

Radice G.L. (2013). N-cadherin-mediated adhesion and signaling from development to disease: lessons from mice. Prog. Mol. Biol. Transl. Sci. 116, 263-289.

Ren Y., Zhou X., Liu X., Jia H.H., Zhao X.H., Wang Q.X., Han L., Song X., Zhu Z.Y., Sun T., Jiao H.X., Tian W.P., Yang Y.Q., Zhao X.L., Zhang L., Mei M. and Kang C.S. (2016). Reprogramming carcinoma associated fibroblasts by AC1MMYR2 impedes tumor metastasis and improves chemotherapy efficacy. Cancer Lett. 374, 96-106.

Shi J., Hou Z., Yan J., Qiu W., Liang L., Meng M., Li L., Wang X., Xie Y., Jiang L. and Wang W. (2020). The prognostic significance of fibroblast activation protein-α in human lung adenocarcinoma. Ann. Transl. Med. 8, 224.

Striefler J.K., Riess H., Lohneis P., Bischoff S., Kurreck A., Modest D.P., Bahra M., Oettle H., Sinn M., Bläker H., Denkert C., Stintzing S., Sinn B.V. and Pelzer U. (2021). Mucin-1 protein is a prognostic marker for pancreatic ductal adenocarcinoma: Results from the CONKO-001 study. Front. Oncol. 11, 670396.

Teichgräber V., Monasterio C., Chaitanya K., Boger R., Gordon K., Dieterle T., Jäger D. and Bauer S. (2015). Specific inhibition of fibroblast activation protein (FAP)-alpha prevents tumor progression *in vitro*. Adv. Med. Sci. 60, 264-272.

Teng C., Zhang B., Yuan Z., Kuang Z., Chai Z., Ren L., Qin C., Yang L., Han X. and Yin L. (2020). Fibroblast activation protein-α-adaptive micelles deliver anti-cancer drugs and reprogram stroma fibrosis. Nanoscale 12, 23756-23767.

Wang Q., Li W., Zhang Y., Yuan X., Xu K., Yu J., Chen Z., Beroukhim R., Wang H., Lupien M., Wu T., Regan M.M., Meyer C.A., Carroll J.S., Manrai A.K., Jänne O.A., Balk S.P., Mehra R., Han B., Chinnaiyan A.M., Rubin M.A., True L., Fiorentino M., Fiore C., Loda M., Kantoff P.W., Liu X.S. and Brown M. (2009). Androgen receptor regulates a distinct transcription program in androgen-independent prostate cancer. Cell 138, 245-256.

Wang K., Zhang W., Wang Z., Gao M., Wang X., Han W., Zhang N. and Xu X. (2020). Flavokawain A inhibits prostate cancer cells by inducing cell cycle arrest and cell apoptosis and regulating the glutamine metabolism pathway. J. Pharm. Biomed. Anal. 186, 113288.

Williams E.D., Gao D., Redfern A. and Thompson E.W. (2019). Controversies around epithelial-mesenchymal plasticity in cancer metastasis. Nat. Rev. Cancer 19, 716-732.

Wu G., Xie B., Lu C., Chen C., Zhou J. and Deng Z. (2020). microRNA-30a attenuates TGF-β1-induced activation of pulmonary fibroblast cell by targeting FAP-α. J. Cell Mol. Med. 24, 3745-3750.

Yan J., Wu Q., Zhao Z., Wu J., Ye H., Liang Q., Zhou Z., Hou M., Li X., Liu Y. and Yin L. (2020). Light-assisted hierarchical intratumoral penetration and programmed antitumor therapy based on tumor microenvironment (TME)-amendatory and self-adaptive polymeric nanoclusters. Biomaterials 255, 120166.

Yang Y.N., Zhang X.H., Wang Y.M., Zhang X. and Gu Z. (2018). miR-204 reverses temozolomide resistance and inhibits cancer initiating cells phenotypes by degrading FAP-α in glioblastoma. Oncol. Lett. 15, 7563-7570.

Ye D.W. and Zhu Y. (2019). Prostate cancer and prostatic diseases Best of China, 2018. Prostate Cancer Prostatic Dis. 22, 1-2.

Accepted February 7, 2022